Optical fiber gratings for structural health monitoring in high-temperature environments

Richard J. Black, Kelvin Chau, George Chen, Behzad Moslehi, Levy Oblea, and Keo Sourichanh
Intelligent Fiber Optic Systems Corporation, 2363 Calle Del Mundo, Santa Clara CA 95054-1008
www.ifos.com

ABSTRACT

Fiber gratings are proving to provide versatile discrete sensor elements for structural health monitoring systems. For example, they outperform traditional resistive foil strain gages in terms of temperature resistance as well as multiplexing capability, relative ease of installation, electromagnetic interference immunity and electrical passivity. However, the fabrication method and post-fabrication processing influences both performance and survivability in extreme temperature environments. In this paper, we compare the performance and survivability when making strain measurements at elevated temperatures for a range of fabrication and processing conditions such as UV-laser and electric-arc writing and post-fabrication annealing. The optimum method or process will depend on the application temperatures (e.g., up to 300°C, 600°C or 1000°C), and times at these temperatures. As well, other sensing requirements, including the number of sensors, measurand and sensitivity may influence the grating choice (short or long period).

Keywords: Fiber optics, optical fiber sensors, fiber gratings, structural health monitoring, high-temperature sensors

1 INTRODUCTION

Optical fibers have the following characteristics that can benefit sensor applications. They (a) are noise free (they are both immune to electromagnetic interference (EMI) and do not generate EMI), (b) are electrically passive and this safe in explosive environments, (c) allow transmission of sensed information over long distances and through difficult to access regions, e.g., through small holes, down oil wells, etc., (d) are small enough to be integrated into smart materials, (d) can be highly durable, are low in weight, and (e) are capable of being installed with less labor than comparable electronics sensors. The writing of optical fiber gratings into select regions along an optical fiber provides a means of creating discrete high-sensitivity, high-resolution sensing sections along the fiber. Optical fiber gratings

Multipoint strain sensing [1-4] is crucial to Integrated Systems Health Management (ISHM) for aerospace structures. Strain sensing with commonly used resistive foil gages is typically restricted to less than 400°C, is subject to electromagnetic interference and installation is labor intensive. By contrast, light-weight fiber optic sensors have the potential for noise-free measurement to much higher temperatures with electromagnetic interference immunity, electrical passivity and thus safety in explosive environments, and remote access. Fiber optic grating sensors are also multiplexable and precise, but standard gratings are subject to high-temperature degradation. However, IFOS is developing special fiber grating based strain sensors that significantly extend the maximum temperature at which accurate strain sensing is achievable to 800°C and beyond, thus filling a particular need for users of high-temperature health monitoring of (a) jet and other high temperature engines, (b) thermal protection systems – including those on leading and trailing edges of aircraft and in re-entry protection for shuttle and other space vehicles, and (c) satellite space vehicles. Further applications include instrumentation for fire warning systems, furnaces, nuclear power plants, high-temperature automotive engine sensors, oil refinery and drilling, chemical sensors, and homeland security sensor systems. While our focus is on reliable high-temperature strain measurements, the system will also have the potential for extension to simultaneous measurement of strain, vibration, acceleration, and temperature, and, with appropriately coated gratings, sensitivity to various chemicals and biochemicals, and applicable to gases in combustion environments and high temperature spectroscopy.

In Section 2, we briefly review grating writing methods, in Section 3, strain testing, in Section 4, temperature cycling, and in Section 5, we conclude.

2 FIBER GRATING WRITING METHODS

Optical fiber gratings most commonly have a periodic variation in refractive index along their length with period Λ that, in silica fiber, is on the order of a half a micron to produce Fiber Bragg Gratings (FBGs) that reflect 1.5 micron light. These Short Period Gratings (SPGs) may be contrasted with so-called Long Period Gratings (LPGs) that have periods on the order of several hundred microns and for which light is lost from the fundamental core mode to forward-propagating cladding modes. Both grating types have dips in transmission spectra of the fundamental mode. However, only SPGs have significant spectral peaks in the reflected spectra.

Grating writing in optical fibers and integrated optic waveguides may be broadly classified into three categories:

1. UV laser photosensitivity-induced inscription – Type I [5-8] and Type II [9-10]
2. IR laser heat-induced inscription
3. Electric-arc heat-induced inscription

Method 1 was developed and patented by UTRC (USA) and CRC (Canada) and now used by many laboratories worldwide having been the focus of thousands of investigations. Type I gratings can start to degrade as temperature is increased over 250°C. Annealing can provide some improvement to the thermal resistance. However, Type II gratings in general have more thermal resistance.

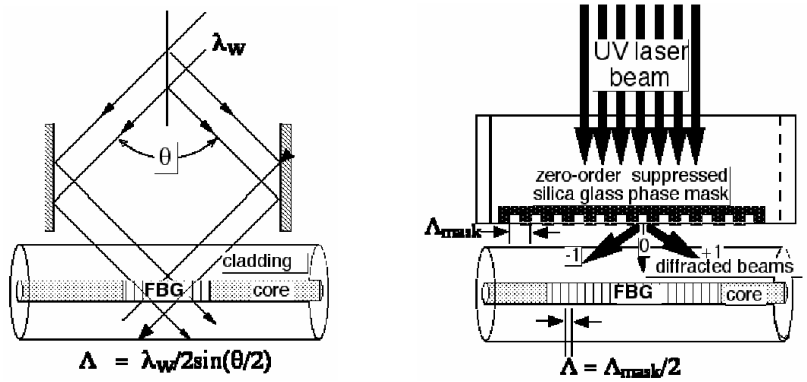

(a) (b)

Fig. 1. UV laser photosensitivity-induced inscription of FBGs: (a) original split interferometer method [5], and (b) phase mask method [8].

Method 2 has been explored by a number of laboratories. Fiber gratings written by periodical local heating of the fiber with Ti:sapphire [13], CO_2 [14-15] and CO [18] laser radiation have demonstrated very high thermal stability.

Method 3: The local heating of the fiber also takes place in the process of grating inscription by electric arc discharges, and their thermal stability must be comparable as well. The electrical arc technique is simpler and does not need expensive laser equipment.

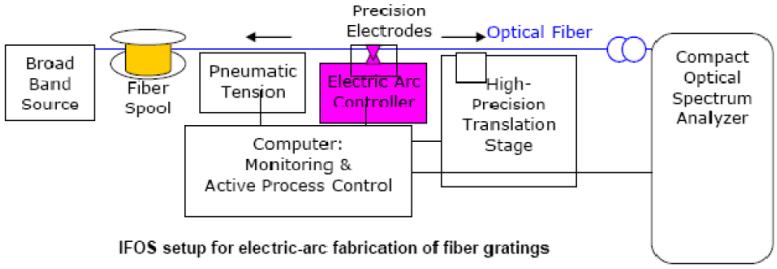

Fig. 2. Simplified schematic of setup used by IFOS for electric arc fabrication of fiber gratings.

In the following sections we discuss measurements made on LPGs fabricated by IFOS using the electric arc method in contrast to standard industrial UV-inscribed SPGs.

3 LOADING TESTS

We performed a series of calibrated strain tests using weight-induced tensile strain. In particular, as shown in Fig. 3 between the spool and a clamp involving large surface area rubber strips attached to an optical fiber containing a grating, just below that grating.

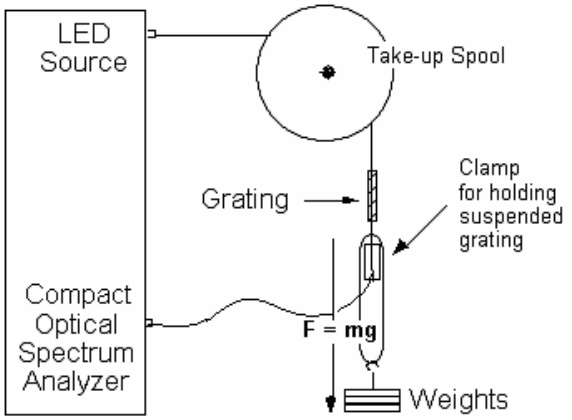

Fig. 3. Calibrated strain measurements of gratings using weights.

Fig. 4 shows the movement of wavelength spectra for increasing weights. As the weight is increased to 235 grams, resulting in a tensile strain of approximately 2000 με, the spectral dip moves by approximately 78 nm shorter wavelength.. Since the dip wavelength is given (Eq. 1) by $\lambda^{(m)} \approx (n_{eff1}-n_{effm})\Lambda$ these results indicate that stretching the grating decreases the effective index difference $(n_{eff1}-n_{effm})$ substantially more than the grating period Λ is increased. We can understand this happening if the stretching acts to significantly reduce the effective index of the fundamental mode, squeezing it somewhat out of the core.

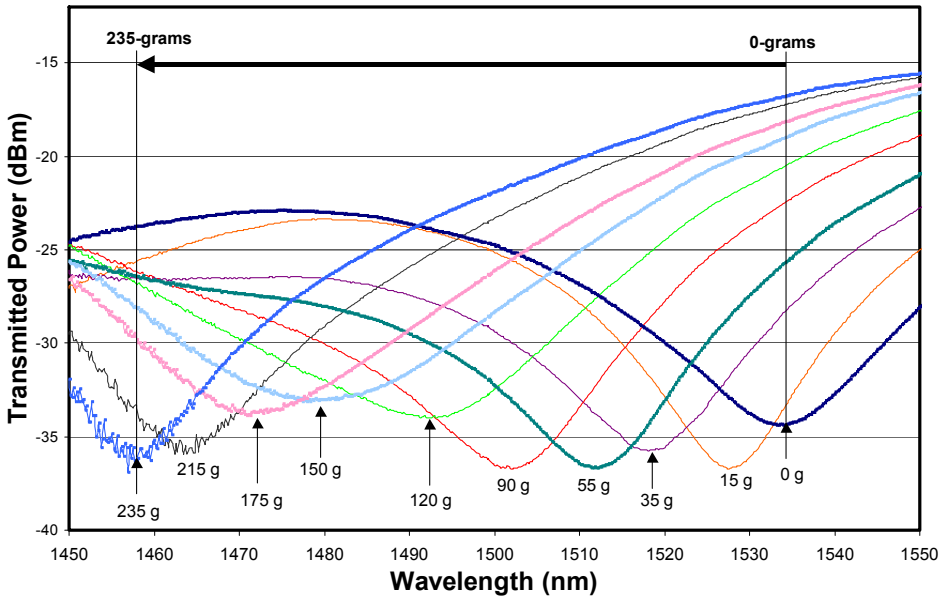

Fig. 4. Transmission spectra for a range of weights used to provide calibrated strain on an IFOS electric-arc fabricated grating.

In Fig. 5, we plot the dip wavelength as a function of weight. (More measurements were taken than those plotted in Fig. 4). We see as shift of -330 pm / gram. It can be shown (see next section) that for a 125 um silica fiber the strain resulting from a hanging weight is approximately 8.53 με/gram. Thus the wavelength shift per unit strain is approximately -39 pm / με (which may be compared with the short-period grating shift at 1550 nm of 1.2 pm / με - see next section for details).

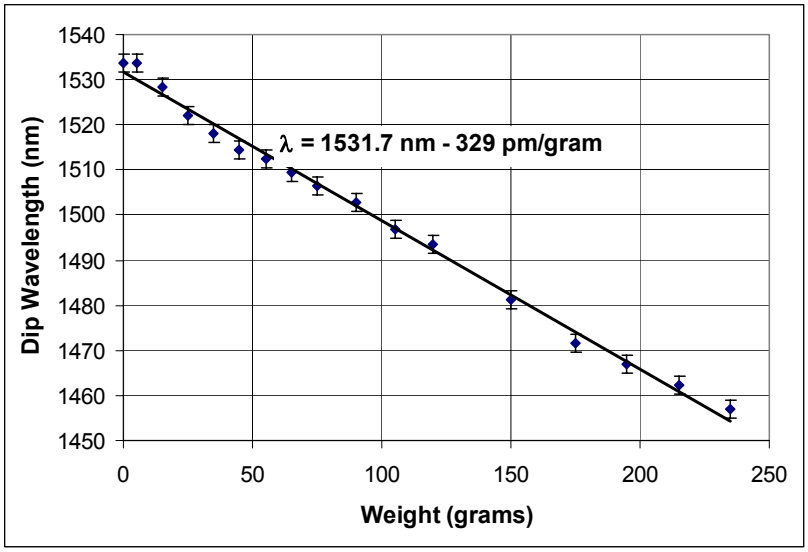

Fig. 5. Dip wavelength versus weight for IFOS electric-arc written Long Period Grating (LPG) showing a shift of approximately -330 pm/gram.

This result may be compared with that for a standard UV-laser written short period grating shown in Fig. 6.

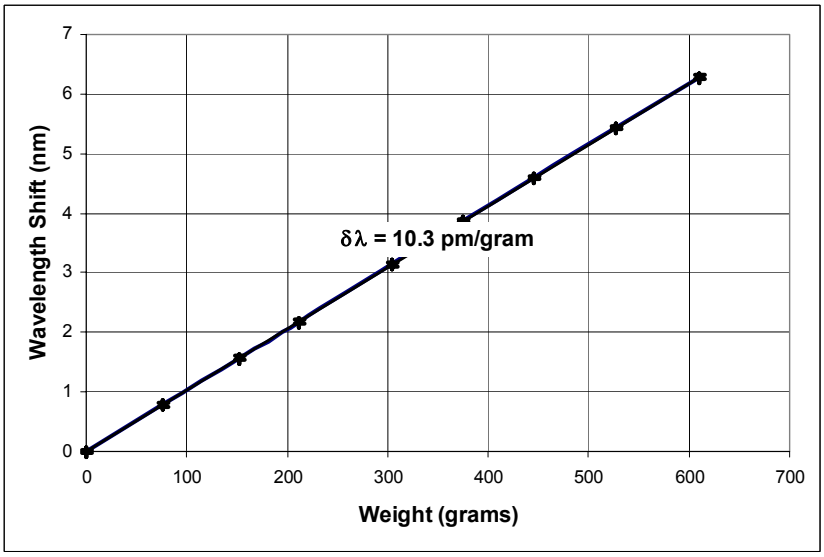

Fig. 6. Dip wavelength versus weight for a standard UV-laser written 1550-nm Short Period Grating showing a shift of approximately 10 pm/gram.

We note that the shift for the electric-arc written long period grating is 33 times larger than that of the UV written short period grating. In addition, while the dip wavelength increases with weight applied strain in the short period case, it decreases for this particular electric arc written long period grating.

4 TEMPERATURE CYCLING TESTS

Fig. 7 shows measurements with the tube furnace cycled between room temperature to 1000°C. We note:

- Survivability and repeatability – when the grating is returned to room temperature, the initial spectrum is retained.
- High temperature operation - significant dips in the spectrum remain at 1000°C and again the result is repeatable (within experimental error - in our initial tests the accuracy of the temperature measurement within the tube furnace is estimated at ±20°C).

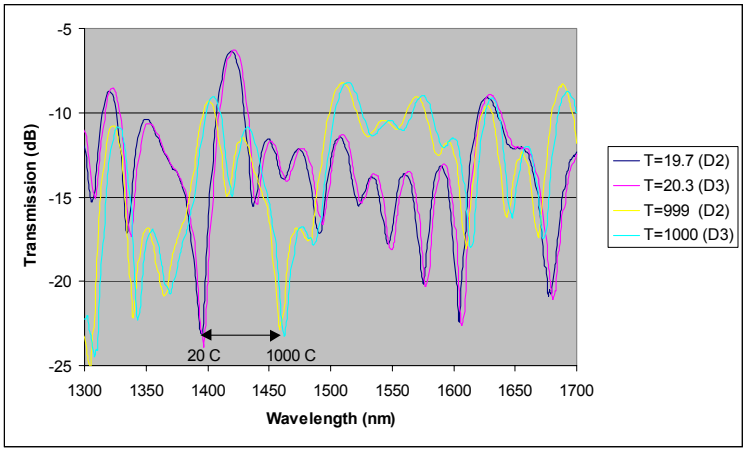

Fig. 7. IFOS electric arc fabricated grating: Room temperature to 1000°C spectral repeatability measurements for a grating fabricated by IFOS using the technique.

These results may be contrasted with those for a standard industrial gratings fabricated with a UV laser shown in Fig. 8.

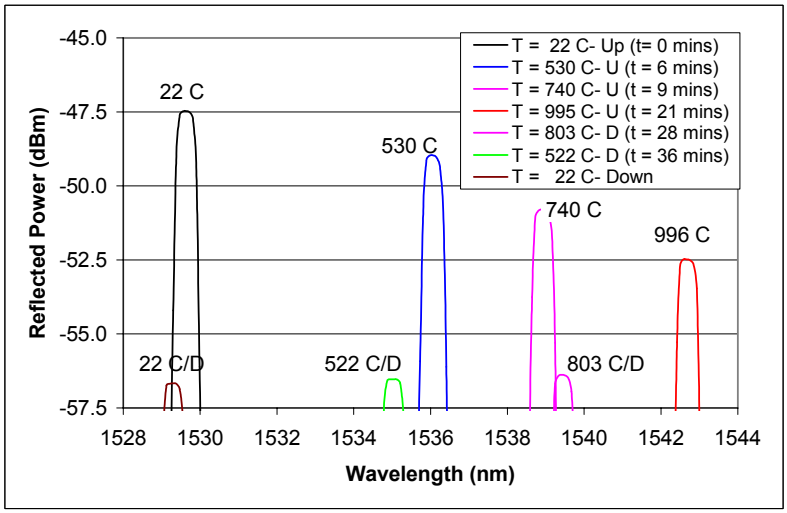

Fig. 8. Standard industrial UV grating: Spectral measurements of reflected power as the grating is heated a second time from room temperature up (U) to 1000°C, and then a further 75°C to 1075°C before it is let to cool down (D).

In this experiment, as for the IFOS gratings in the previous experiment, we heated the standard grating up to nearly 1000°C with the tube furnace on maximum, and then let it cool back down to room temperature. Note that as the grating was heated to 996°C in 21 minutes its reflectivity decreased approximately by 5 dB. It continued to degrade in the high temperature by another 3.5 dB as it cooled to 803°C over the next 7 minutes. As it cooled further, it appeared to stabilize indicating that the degradation mechanisms occurring below 800°C had been removed in the initial heating – however in removing these, the reflectivity had decreased by nearly a factor 8. As shown in Fig. 9further cycling up to 1000°C in 20 minutes reduced the reflectivity by another 3.5 dB. Heating the tube furnace a further 75°C to 1075°C took a further 87 minutes and virtually destroyed the reflectivity – i.e. reduced it by another 9 dB to make it 22.5 dB lower than the original starting value in Fig. 8.

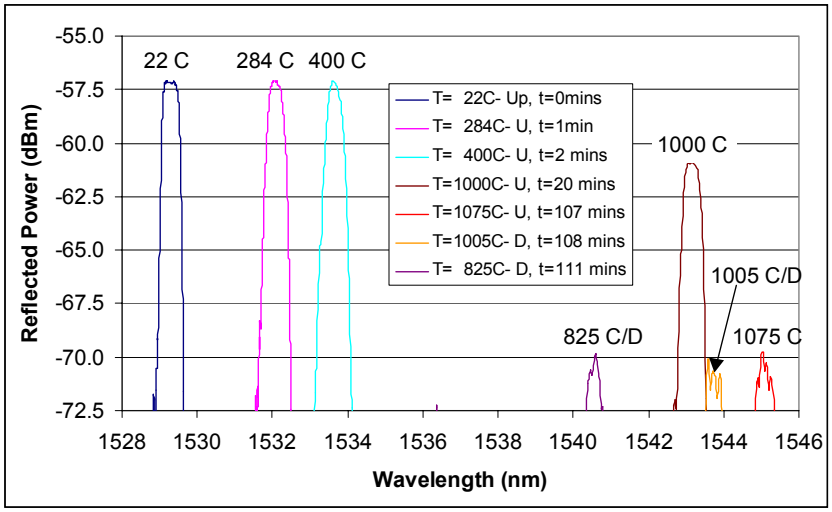

Fig. 9. Standard industrial UV grating: Spectral measurements of reflected power as the grating is heated a second time from room temperature up (U) to 1000°C, and then a further 75°C to 1075°C before it is let to cool down (D).

5 LOADING TESTS AT ELEVATED TEMPERATURES

In Fig. 10, we show experimental results for the strain dependence of an example electric arc fabricated LPG at room temperature and at 650°C. We note that the increased temperature shifts the wavelength versus weight curve to longer wavelengths.

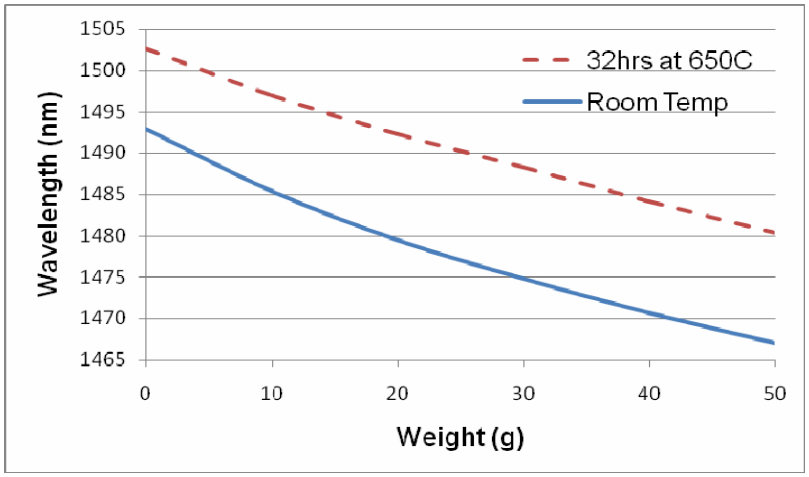

Fig. 10. Strain test results for spectral dip wavelength versus applied weight at room temperature and 650 °C.

6 CONCLUSIONS

Electric-arc inscription provides a method for fabricating long-period gratings that are stable to high temperatures. We successfully fabricated a series of high-temperature gratings using this method. The electric-arc written gratings were characterized as a function of wavelength, strain and temperature. A strain response 33 times larger than that of standard UV-laser written short period gratings was obtained. While the shift for these standard gratings is on the order of 1 picometer per microstrain, for electric-arc written long-period there can be substantial variability dependent on fabrication details. This has the potential for leading to a rich range of sensors and filters.

APPENDIX: STRAIN RELATIONSHIPS FOR SHORT–PERIOD GRATINGS

When a fiber is stretched the tensile strain ε is related to applied force F via the Young's modulus E and the cross-sectional area A, i.e.,

$$\varepsilon = F \,/\, (E_{silica}\, A_{fiber}) \tag{1}$$

For fiber diameter, 125 μm, given the Young's modulus for silica,

$$E_{silica} \approx 94\ \{1+3\ \varepsilon\}\ \text{GPa} \approx 9.4 \times 10^{10}\ \text{Nm}^{-2}, \tag{2}$$

we obtain

$$\varepsilon / F = 1/ (E_{silica}\, A_{fiber}) \approx 0.087\ \%\ /\ \text{N} = 0.87\ \mu\varepsilon\ /\ (\text{gram.m.s}^{-2}), \quad (\varepsilon << 1) \tag{3}$$

Taking F = mass.g = mass.9.8 m.s^{-2}.

$$\boxed{\varepsilon / mass \approx 8.53\ \mu\varepsilon/\text{gram}} \tag{4}$$

For standard **short-period gratings,** fractional wavelength shift is related to strain via the photo-elastic coefficient for silica, $p_e \approx 0.22$, as follows:

$$\delta\lambda_B/\lambda_B \approx (1 - p_e)\ \varepsilon \approx 0.78\ \varepsilon \tag{5}$$

Thus

$$(\delta\lambda_B/\lambda_B)\ /\ F \approx 0.068\ \%\ /\ \text{N}, \tag{6}$$

and

$$(\delta\lambda_B/\lambda_B)\ /\ mass \approx 0.00665\ \%\ /\ \text{gram} \tag{7}$$

At 1300 nm

$$\delta\lambda_B / F \approx 0.88\ \text{nm / N},\ \delta\lambda_B / \varepsilon \approx 1.01\ \text{pm / } \mu\varepsilon,\ \text{and}\ \delta\lambda_B / mass \approx 8.7\ \text{pm / gram} \tag{8}$$

At 1550 nm

$$\delta\lambda_B / F \approx 1.05\ \text{nm / N},\ \delta\lambda_B / \varepsilon \approx 1.21\ \text{pm / } \mu\varepsilon,\ \text{and}\ \delta\lambda_B / mass \approx 10.3\ \text{pm / gram} \tag{9}$$

REFERENCES

Standard Fiber Bragg Grating Sensors

1. B Moslehi, RJ Black, K Toyama, HJ Shaw, “Multiplexible Fiber-Optic Strain Sensor System with Temperature Compensation Capability”, US Patent issued Aug. 2003, filed March 1999, IFOS, USA.
2. BA Childers, ME Froggatt, SG Allison, TC Moore, Sr.; DA Hare, CF Batten, DC Jegley, “Use of 3000 Bragg grating strain sensors distributed on four eight-meter optical fibers during static load tests of a composite structure”, Proc. SPIE, 8th International Symposium on Smart Structures, March 4-8, 2001, Newport Beach, California.
3. JM Seim, WL Schulz, E Udd, M Morrell, “Higher-speed demodulation of fiber grating sensors, Proc. SPIE Vol. 3670, p. 8-15, Smart Structures and Materials 1999: Sensory Phenomena and Measurement Instrumentation for Smart Structures and Materials, Richard O. Claus; William B. Spillman; Eds 5/1999
4. MC Mowlem, A Chambers, JP Dakin, “Development of sensor technology to facilitate in-situ measurement of damage in composite materials for spacecraft applications”, Proc. SPIE Vol. 4234, p. 144-151, Smart Materials, Alan R. Wilson; Hiroshi Asanuma; Eds. 4/2001

UV Laser Photo-induced (Standard) Gratings

5. GR Meltz, WW Morey, WH Glen, “Formation of Bragg Gratings in Optical Fibers by a Transverse Holographic Method,” Opt. Lett., 14, pp. 823-825, 1989.
6. WW Morey et al, Optics & Photonics News (Feb.), 8 (1994).
7. G Meltz, OFC/IOOC'93 - Tutorial, 360 (1993).
8. KO Hill, B Malo, F Bilodeau, DC Johnson, “Photosensitivity in Optical Fibers,” Ann. Rev. Mater. Sci., 125, 1993.
9. PSJ Russell, J-L Archambault et al, Physics World (Oct.), 41 (1993).
10. JL Archambault et al., "100% reflectivity Bragg reflectors produced in optical fibres by single excimer laser pulses", Electron. Lett. 29, 453 (1993).
11. AI Gusarov, DB Doyle, “Contribution of Photoinduced densification to refractive-index modulation in Bragg gratings written in Ge-doped silica fibers”
12. HG Limberger, PY Fonjallaz, RP Salathé, F Cochet, Appl. Phys. 68, 3069 (1996)

Ultrafast Ti:sapphire 800 nm Laser-Written Gratings

13. D Grobnic, C W Smelser, S J Mihailov and R B Walker , “Long-term thermal stability tests at 1000 °C of silica fibre Bragg gratings made with ultrafast laser radiation”, 2006 Meas. Sci. Technol. 17 1009-1013 (2006).

CO_2 Laser Heat-Written Gratings

14. L Drozin, P-Y Fonjallaz, L Stensland, "Long-period fibre gratings written by CO2 exposure of H2-loaded, standard fibres", ***Electronics Letters*** 36(8), p. 742, (2000).
15. Yinian Zhu, Ping Shum, Hin-Joo Chong, M. K. Rao, Chao Lu, “Strong resonance and a highly compact long-period grating in a large-mode-area photonic crystal fiber”, Opt. Express 11, 1900-1905 (2003), http://www.opticsexpress.org/abstract.cfm?URI=OPEX-11-16-1900.
16. DD Davis, TK Gaylord, EN Glytsis, SC Mettler, “Very high-temperature stable CO2-laser-induced long-period fiber gratings,” Electron. Lett., vol. 35, pp. 740–742, Apr. 29, 1999.
17. DD Davis, TK Gaylord, EN Glytsis, SC Mettler, “CO laser-induced long-period fiber gratings: Spectral characteristics, cladding modes and polarization independence,” Electron. Lett., vol. 34, pp. 1416–1417, July 9, 1998.

CO Laser Heat-Written Gratings

18. VI Karpov, MV Grekov, EM Dianov, KM Golant, SA Vasiliev, OI Medvedkov, RR Khrapko, “Mode-field converters and long-period gratings fabricated by thermodiffusion in nitrogen-doped-silica-core fibers,” in Proc. Mater. Res. Soc. Symp., vol. 531, 1998, pp. 391–396.

Electric-Arc-Written (High-Temperature) Gratings

19. RJ Black, K Chau, K Good, M Hernandez, L Oblea, J Straub, B Moslehi, “Fiber-Optic Sensing for Thermal Protection Structures in Vehicle Health Monitoring”, Book of Abstracts for QNDE 2005 - Review of Progress in Quantitative NDE (2005), Bowdoin College, Maine.
20. N Godbout, X Daxhelet, A Maurier, S Lacroix, “Long-period fiber grating by electrical discharge,” ECOC'98 p 397, 1998.
21. G Rego, O Okhotnikov, E Dianov, V Sulimov, “High-temperature stability of long-period fiber gratings produced using an electric arc”, J. Lightwave Tech. 19(10), 1574 (2001).
22. A Malki, G Humbert, Y Ouerdane, A Boukhenter, A Boudrioua, “Investigation of the Writing Mechanism of Electric-Arc-Induced Long-Period Fiber Gratings”, Applied Optics-OT, 42(19), 3776-3779, July 2003.